hydrothermal method and coated with silica at room temperature for high biocompatibility that published in our previous works [10]. The potential of doxorubicin against the resistant leukemia cancer cells, K562 was evaluated using the MTT assay. The DOX loaded FA/SiO_2@ZnO NRs present several interesting properties that are favorable for use in drug targeting: conventional DOX. This gain in antineoplastic activity could be due to the vectorization of the drug. Indeed, when DOX is brought to the cell by a vector, this may change its route of internalization and zones of accumulation in the cell. It was reported that DOX can change its intracellular distribution when it is bound to an entity, for example as conjugated to polymers [11] or cell penetrating peptides [12]. These distribution changes are most of the time
correlated to differences in cytotoxicity between conventional and vectorized DOX.

Materials and Methods

Materials

Dicyclohexylcarbodiimide (DCC) and folic acid were received from Merck chemical company and used without any further purification. Deionized and distilled water was used for the preparations in this work. Doxorubicin hydrochloride (DOX, Aldrich) was used for the drug loading and purchase from farmacia Italia Company.

Synthesis of folic acid/SiO2@ZnO nanorod conjugate.

ZnO nanorods with average size of 21×200 nm were prepared by a facile and simple hydrothermal route. Coating of the particles with silica were done by TEOS and APTMS in room temperature for enhanced biocompatibility [10]. For assembling of folic acid (FA) to SiO_2 coated ZnO nanorods, 0.12 g of folic acid and 0.06g of dicyclohexylcarbodiimide (DCC) sonicated in 30 ml DMF for 1hour up to dissolving all solid materials. The obtained solution and 0.06 g of nanorods was stirred in room temperature for about 15 hours. The resulted yellow solid (FA/SiO2@ZnO conjugate) was then washed with deionized water and dried during 2 days in the labrotary.

Synthesis of Doxorubicin (DOX) drug loaded silica coated ZnO nanorod.

The water-soluble anti-cancer drug doxorubicine was chosen as a model drug. The DOX loading was carried out by dispersing 0.06g of FA/SiO2@ZnO conjugate and DOX (3mg) in 30 ml DMF. The mixture was stirred for 24 hours to facilitate DOX uptake. The optical density of residual DOX in the supernatant was measured at 480 nm by UV–Vis spectrophotometer. The drug loaded nanoparticles were then separated, washed several times with distilled water and dried in room temperature.

Cytotoxicity assays (MTT assay)

Prior to the experiment, the leukemia cancer cells, K562, were seeded in standard 96-well plates at $2 * 10^4$ cells per well and grown for 24 h. The culture medium was then discarded and cells were treated for 24 and 48 hours with 0.0, 0.65, 1.25, 2.5 and 5mg/mL of nanocariers contained doxorubicin drug. The effect of DOX and DOX-loaded nanocarriers on the cell viability were assessed using a tetrazolium dye (3-(4, 5-dimethy-lthiazol-2-yl)-2,5diphenyltetrazolium bromide, named MTT assay. The medium containing DOX was discarded and cells were rinsed thrice with phosphate buffered saline (PBS). They were incubated during 4 h with a 0.5 mg/mL MTT solution in culture medium. Then the medium was replaced by 200 µL of DMSO to dissolve the formazan crystals formed by viable cells and the percentage cell viability (%) compared to vehicle-treated control cells. Arbitrary assigned 100% viability was determined by measuring absorbance at 480 nm.

Results and Discussion

FTIR Study

Fig 1. a. and scheme 1 is shown bonding between carboxyl group of FA (folic acid) and amino group on the surface (NH2 groups of APTMS) of the nanorods by the peaks in 16801700 cm^{-1} (C=O stretching of amide bond) and 1580-1610 cm^{-1} (N-H stretching of amid bond). Folic acid characteristic peaks in 1483, 1605 and 1696 cm^{-1} in Fig. 1 b also exist in the FTIR spectra of the FA conjugated NRs (fig 1. a). FTIR spectra of pure DOX and DOX loaded silica coated nanorods are presented in Fig. 2. a and b.

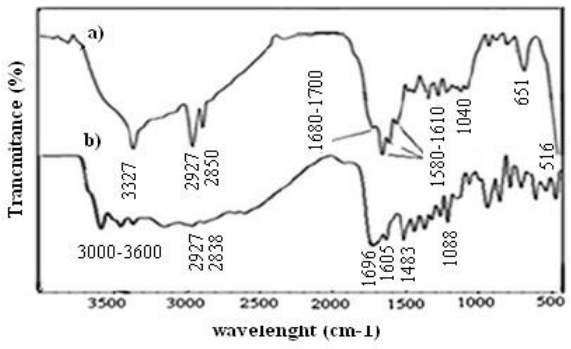

Figure 1. FTIR spectra of (a) FA/SiO2@ZnO NRs (b) pure FA.

FTIR spectrum of pure DOX shows peaks at 3382 cm^{-1} due to N–H and O-H stretching vibrations for

the primary amine structure. The structure of doxorubicine and its binding manner to DNA is shown in fig. 3. The bands observed at 891 cm^{-1} and 782 cm^{-1} due to N–H wag in pure DOX appear in the FTIR spectrum of DOX-conjugated nanorods. From this FTIR results, it can be interpreted that attachment of DOX to the silica coated nanorods occurs by electrostatic intractions because N-H and O-H bonding in about 3300-500 cm^{-1} are not changed.

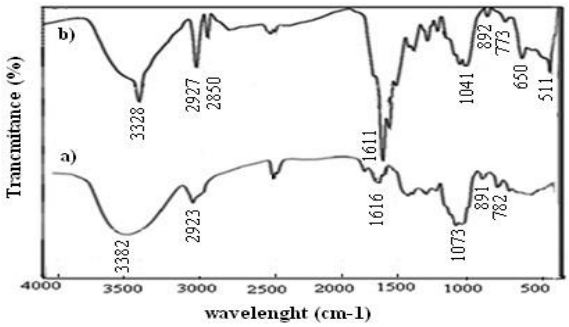

Figure 2. FTIR spectra of (a) pure DOX (b) DOX loaded silica coated NRs.

Table 1. List of FTIR spectra for pure FA, pure DOX, FA/SiO2@ZnO NRs and DOX-FA/SiO2@ZnO NRs

Freq. assignments	Pure FA (cm^{-1})	FA/SiO_2 @ ZnO NRs (cm^{-1})	Pure DOX (cm^{-1})	DOX-FA/SiO2@ZnO NRs (cm^{-1})
ν(Zn-O)	---	516	---	511
ν (Zn-O-Si)	---	651	---	650
ω (N-H)	---	---	782,891	773,892
δ (O-H, N-H)	1605,1696	---	1616	1611
ν (C-O)	1088	1040	1073	1041
ν (N-H) amide I region	---	1580-1610	---	---
ν (C=O) amide II region	---	1680-1700	---	---
ν (C-H)	2838, 2927	2850,2927	2923	2850, 2927
ν (O-H), ν (N-H)	3000-3600	3327	3382	3328

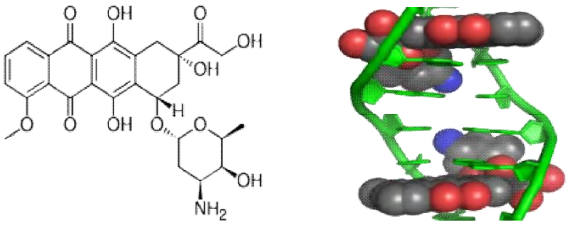

Figure 3. Doxorubicin chemical structure (left) and its binding manner to DNA (right).

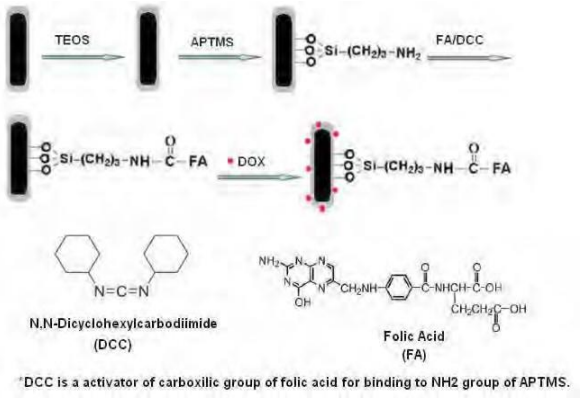

Scheme 2. Attachment of DOX and folic acid to the as prepared SiO2@ZnO NRs.

UV/Visible study

The prepared conjugated nanorods were first dispersed in distilled water by ultrasonication and then the UV-Vis optical absorption characteristics of the sample were measured. The peaks in 285 nm in figure 4. a is due for assembling of folic acid on NRs surface by formation of amide bonding between them. Pure folic acid has an absorbtion peak in 283 nm. After the doxorubicine were loaded with DOX, the UV-Vis peaks at around 237 and 482 nm attributing to the loaded DOX molecules were observed by the UV-Vis spectrum in Fig 4.b, which were slightly shifted from the corresponding absorption peaks of free DOX molecules at 233, 253 and 481 nm, respectively. Fig 4.c and 4.d represent the UV-Vis spectrum of pure FA and DOX respectively. The slight shifts of the spectra may be originated from the interaction of the loaded DOX drugs and the conjugated components. All these results demonstrated that DOX molecules were successfully loaded onto the NRs via the efficient interaction between the drug molecules and drug-carriers.

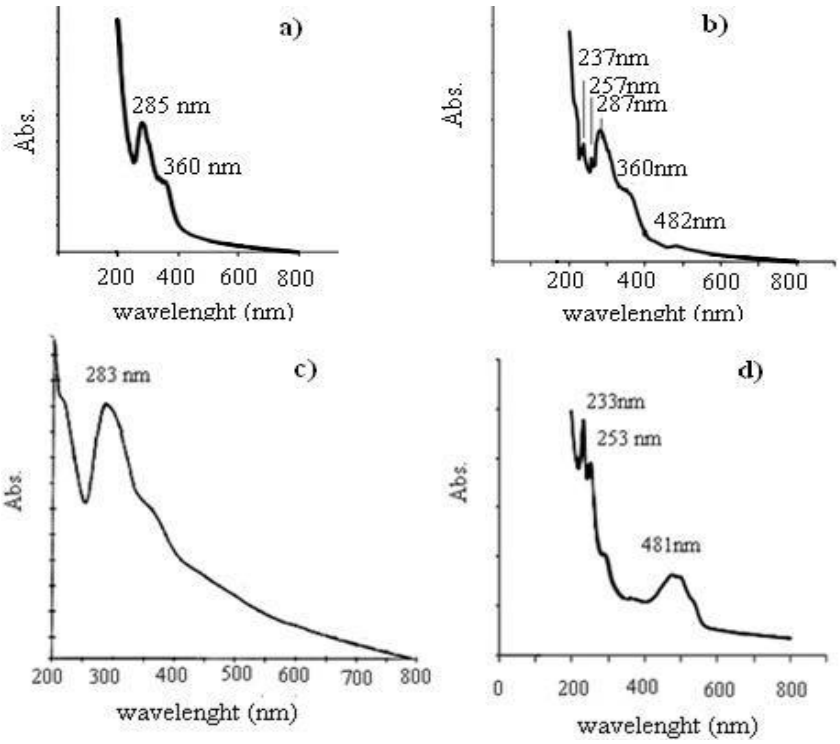

Figure 4. UV-Vis spectra: a) FA/SiO2@ZnO NRs b) DOX loaded FA/SiO2@ZnO NRs c) pure FA d) pure DOX

Cytotoxicity of DOX-loaded FA/SiO2@ZnO NRs on K562 cells

We studied the cytotoxicity of our DOX-FA/SiO2@-NRs and pure DOX suspensions at Different drug concentrations. The results presented in Fig. 5 show that, within 24 h, the DOX- FA/SiO2@ZnO NRs suspension was significantly more active against K562 cells than pure DOX solution. The NRs alone has no significant cytotoxic effect on K562 cells, while DOX- FA/SiO2@NRs induced higher cell mortality than conventional drug. Cell viability reached nearly 21%, whereas DOX in solution led to only 40% viability at the concentration of 5 mg/ml. These data indicate that the intracellular action of internalized DOX-FA/ SiO2@ZnO NRs plays an important role in the gain of cytotoxicity. Fig. 6 and table 2 show the result of dose dependence cytotoxicity of DOX and DOX-FA/ SiO2@ZnO NRs against leukemia cancer cells, K562 line within 24 h. The NRs are deposited at greater than 24 hours so the experiments were carried out during this time.

The morphology and behavior of DOX-FA/SiO2@ZnO NRs against leukemia cancer cells, K562 cultured in vitro was observed under phase-contrast microscope and evaluated by MTT assays. The phase-contrast micrographs obtained in figure 7 a and b show cell attachments on the DOX-FA /SiO2@ZnO NRs after culture for 24h at concentration 5 mg/ml.

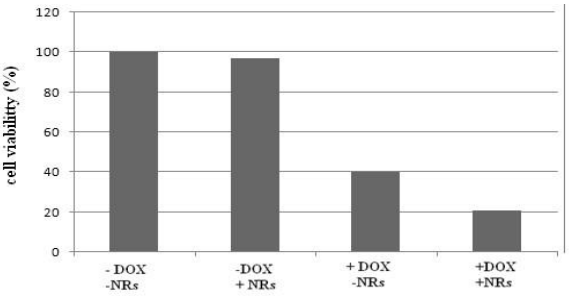

Figure 5. The percentage K562 cells viability (%) for DOX, conjugated NRs and DOX loaded NRs at the concentration of 5 mg/mL within 24 h compared to the vehicle-treated control cells.

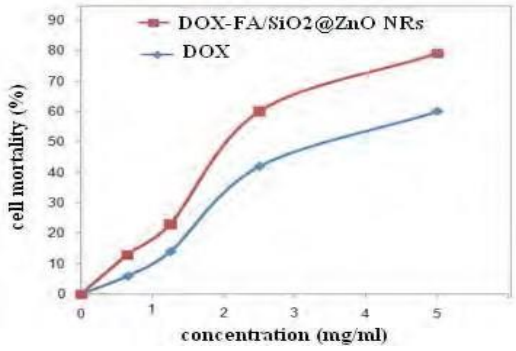

Figure 6. Compare effect of DOX- FA/SiO2@ZnO NRs and DOX at different concentration for 24 h.

Table 2. Dose dependence cytotoxicity at different concentrations for 24.

Concentration (mg/ml)		0	0.65	1.25	2.5	5
Cell mortality (%)	DOX- FA/SiO2@ZnO NRs	0	13	23	60	79
	DOX	0	6	14	42	60

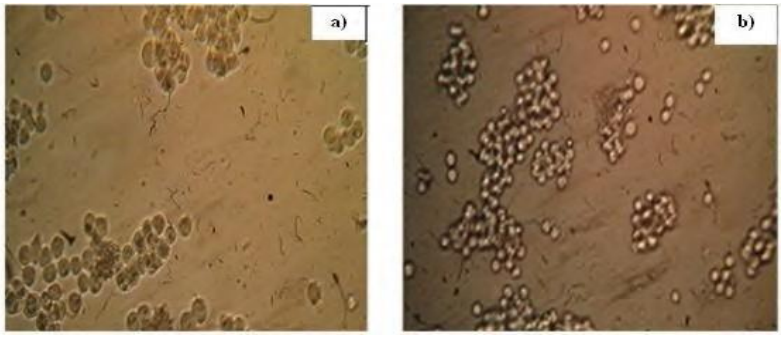

Figure 7. Phase contrast micrographs of K562 cells a) before and b) after incubation with DOX loaded NRs for 24h at concentration 5 mg/ml.

Conclusion

nanocarriers consisting of ZnO nanorods synthesized by hydrothermal method and subsequently coated with SiO_2 (TEOS and APTMS) to reach high biocompatibility. Folic acid molecules were attached to the nanoparticles by the amide bonding to gain more internalization into cancer cells and high efficiency of the nanocarriers. Characterization of the prepared nanocarriers was performed using FTIR and UV-visible techniques. Attachment of the DOX molecules to the NRs via electrostatic interaction was confirmed by FTIR analysis. The NRs was not cytotoxic to the K562cells, while DOX loaded FA/SiO2@ZnO NRs induced higher cell mortality than conventional drug. The cytotoxicity findings by MTT assay indicate that the intracellular action of internalized DOX-FA/SiO_2@ZnO NRs plays an important role in the gain of higher cytotoxicity. The present data show that DOX loaded nanorod is promising for new method in the field of targeted drug delivery.

References

1) Leonard R.C.F., Williams S., Tulpule A., Levine A.M., Oliveros S. 2009. Improving the therapeutic index of anthracyclines chemotherapy: focus on liposomal doxorubicin (Myocet _). *Breast* 18: 218–224.

2) Munnier E., Cohen-Jonathan S., Herve´ K., Linassier C., Souce M., Dubois P., Chourpa I. 2011. Doxorubicin delivered to MCF-7 cancer cells by superparamagnetic iron oxide nanoparticles: effects on subcellular distribution and cytotoxicity, *J Nanopart Res*. 13: 959–971.

3) Weitman S.D., Weinberg A.G., Coney L.R., Zurawski V.R., Jennings D.S., Kamen B.A. 1992. Cellular localization of the folate receptor: potential role in drug toxicity and folate homeostasis, *Cancer Res.* 52: 6708–6711.

4) Reddy J.A., Low P.S. 2000. Enhanced folate receptor mediated gene therapy using a novel pH-sensitive lipid formulation, *J. Control. Release*, 64: 27–37.

5) Horowitz A.T., Goren D., Tzemach D., Mandelbaum- Shavit F., Qazen M.M., Zalipsky S. 1999. Targeting folate receptor with folate linked to extremities of poly(ethylene glycol)-grafted liposomes: in vitro studies, *Bioconjug. Chem.* 10: 289– 298.

6) Guo W., Lee T., Sudimack J.J., Lee R.J. 2000. Receptor-specific delivery of liposomes via folate–PEG–chol, *J. Liposome Res.*10 179– 195.

7) Lu Y., Low P.S. 2002. Folate targeting of haptens to cancer cell surfaces mediates immunotherapy of syngeneic murine tumors, *Cancer Immunol. Immunother*. 51: 153–162.

8) Lee R.J., Low P.S. 1995. Folate-mediated tumor cell targeting of liposome-entrapped doxorubicin in vitro, *Biochim. Biophys. Acta,* 1233: 134–144.

9) Cummings J., McArdle C.S. 1986. Studies on the in vivo disposition of adriamycin in human tumors which exhibit different responses to the drug, *Br. J. Cancer,* 53: 835– 838.

10) Zare K., Molahasani N., Farhadyar N., Sadjadi M.S. 2013. Enhanced Blue Green Emission of ZnO Nanorods Grown by Hydrothermal Method, *Journal of Nano Research,* 21: 43-49.

11) Hovorka O., St'astny M., Etrych T., Subr V., Strohalm J., Ulbrich K., Rihova B. 2002. Differences in the intracellular fate of free and polymer-bound doxorubicin, *J Control Release* 80: 101–117.

12) Aroui S., Brahim S., De Waard M., Bre´ard J., Kenani A. 2009. Efficient induction of apoptosis dy doxorubicin coupled to cell-penetrating peptides compared to unconjugated doxorubicin in the human breast cancer cell line MDAMB 231. *Cancer Lett* 285: 28–38.